

See discussions, stats, and author profiles for this publication at: <https://www.researchgate.net/publication/362027621>

# Physics Evaluation of Alternative Uranium-Based Oxy-Carbide Annular Fuel Concepts for Potential Use in Compact High-Temperature Gas-Cooled Reactors

Article in *Journal of Nuclear Engineering and Radiation Science* · July 2022

DOI: 10.1115/1.4055009

---

CITATIONS

3

READS

148

2 authors, including:



**Blair Bromley**

Canadian Nuclear Laboratories (since 2014; formerly AECL Chalk River Laboratories 1952-2014)

172 PUBLICATIONS 568 CITATIONS

[SEE PROFILE](#)

# Physics Evaluation of Alternative Uranium-based Oxy-Carbide Annular Fuel Concepts for Potential Use in Compact High-Temperature Gas-cooled Reactors

1 \*Wojtaszek, Daniel T. (Lead Author, and Corresponding Author), Daniel.Wojtaszek@cnl.ca  
2 Bromley, Blair P. (Co-Author), Blair.Bromley@cnl.ca

3

4 Canadian Nuclear Laboratories (CNL)

5 286 Plant Rd., Chalk River, ON

6 Canada K0J 1J0

7 \*Lead & Corresponding Author

8

## 9 **ABSTRACT**

10 *Lattice physics calculations have been carried out to evaluate the performance and safety characteristics of a*  
11 *modified high temperature gas-cooled reactor (HTGR) prismatic fuel block concept, based on the MHTGR-350*  
12 *benchmark problem. Key changes were to replace the conventional Tri-Structural ISotropic (TRISO)-filled fuel*  
13 *compacts with heterogeneous, multi-layer annular fuel pellets made with UCO, ThCO, or (U,Th)CO. These fuel*  
14 *pellets have multiple protective cladding layers of pyrolytic carbon and silicon carbide, which will give it robust*  
15 *qualities. With the increased loading of U-235 in the fuel block, it was necessary to replace up to 78 fuel holes and*  
16 *42 coolant holes with a hydrogen-based moderator ( $^7\text{LiH}$ ), in order to ensure a thermal neutron energy spectrum in*  
17 *the lattice. Calculation results demonstrate that the modified fuel concept has several advantages and some*  
18 *challenges relative to the conventional MHTGR-350 design concept. With the increased uranium loading, and the*  
19 *reduced neutron leakage due the use of  $^7\text{LiH}$  moderator rods, higher burnup levels and lower natural uranium*  
20 *consumption levels can be achieved with the same level of uranium enrichment. In addition, the expected fuel*  
21 *residence time increased by a factor of 20 or more, making such a concept very attractive for use in small, modular,*  
22 *“nuclear battery” HTGRs that would only need to be fueled once. Calculation results for the current concept indicate*

23 *positive graphite and hydrogen moderator temperature coefficients, and further modifications will be required to*  
24 *ensure a negative power coefficient of reactivity.*

## 25 **1. INTRODUCTION**

26 There is interest among governments, industry, and reactor vendors in the deployment of small  
27 modular high temperature gas-cooled reactors (SM-HTGRs) [1], [2], [3], [4] for various  
28 applications. The HTGRs that are currently under development use helium gas as the primary  
29 coolant, and are moderated using graphite. Thus, HTGRs can operate at temperatures ( $\geq 700^{\circ}\text{C}$ )  
30 that are much higher than in water-cooled reactors such as pressurized water reactors (PWRs)  
31 and pressure tube heavy water reactors (PT-HWRs). With high operating temperatures, HTGRs  
32 are well-suited for providing heat for a wider range of industrial processes and for higher  
33 efficiency electrical power generation. A drawback for most HTGRs currently under  
34 development, especially those with small cores, is their relatively high neutron leakage, and  
35 their high fissile fuel consumption, which is much higher per unit energy generated than that of  
36 PWRs [7], or PT-HWRs [8], [9], [10]. Their higher fissile consumption is primarily a consequence  
37 of using tri-structural isotropic (TRISO) fuel particles and graphite moderator, which gives a  
38 relatively low loading density of uranium. Hence, higher enrichments of uranium (typically  
39 between 10 wt.% U-235 and 19.75 wt.% U-235) are needed to get sufficiently high burnup  
40 levels and fuel residence time / operating life in an SM-HTGR core.

41 A TRISO particle is composed of a spherical kernel of fissionable material that is surrounded by  
42 layers of graphite and SiC, and is less than 0.1 cm in diameter. TRISO particles have been  
43 designed to be very robust, tough, and durable, performing very well in retaining fission  
44 products (FP) under postulated accident conditions. A small HTGR core comprises hundreds of

45 millions of TRISO particles, the manufacture of which presents challenges, especially with  
46 respect to quality control, for such small particles. Since TRISO particles comprise ~12 vol.%  
47 fissionable material, the use of TRISO particles also limits the mass of fissionable material that  
48 can be loaded in the core, which in turn necessitates the use of higher fuel enrichments, and  
49 limits fuel residence time.

50 An alternative to TRISO particles that is proposed in this study is a multi-layer heterogeneous  
51 annular fuel element that is in the order of 1 cm in diameter and several centimetres long. It is  
52 somewhat similar to a conventional fuel element used in PWRs and PT-HWRs, but as a  
53 modification, it uses additional protective layers to prevent the migration of FPs. Drastically  
54 fewer of such fuel elements would be required in the core, and they could be designed to  
55 enable the loading of a higher volume and mass of fissionable material in the core. Such fuels  
56 retain the multi-layer barrier feature of TRISO fuels, in that multiple coatings are used to help  
57 retain FPs. The performance of the alternative fuel element concept with respect to FP  
58 retention is not evaluated in this study, but may be the topic of future studies.

59 The higher loading of fissionable material in the core requires augmenting neutron moderation  
60 to achieve sufficient fuel burnup and residence time. In this study, elements comprising lithium  
61 hydride (LiH) encased in silicon carbide are added to the fuel block in place of some of the fuel  
62 compacts and coolant holes to provide extra moderation. LiH (using 99.995 at.% Li-7/Li) has  
63 previously been investigated as a moderator for small reactors, especially for space  
64 applications, due to its thermal stability, the moderating characteristics of hydrogen, and the  
65 relatively low neutron capture cross-section of lithium-7 [6].

66 The purpose of this study is to evaluate the impacts on fuel consumption and reactivity  
67 coefficients of using the proposed annular fuel elements in a representative HTGR, the  
68 MHTGR-350 [11], [12], [13], as an alternative to using fuel compacts made of thousands of  
69 TRISO particles in a graphite matrix. This study relies on infinite lattice physics calculations and  
70 a 2-group neutron diffusion leakage model with geometric buckling in-lieu of full core  
71 calculations. The proposed annular fuel element is analyzed with different levels of uranium  
72 enrichment and with uranium-thorium fuel perturbations.

73

74 **2. HTGR FUEL CONCEPTS**

75 **2.1 REFERENCE PRISMATIC FUEL BLOCK**

76 The reference concept is a prismatic fuel block based on the MHTGR-350 (350 MWth / 165  
77 MWe), which is the basis of an international benchmark exercise for prismatic block HTGRs  
78 [11]. The MHTGR-350 uses prismatic fuel blocks (analogous to fuel assemblies in PWRs, and fuel  
79 bundles in PT-HWRs) made of graphite, with holes for coolant (such as helium) and holes for  
80 fuel compacts (which are analogous to fuel elements). The fuel compacts are made of TRISO  
81 particles embedded in a surrounding graphite matrix. Neutron moderation is provided by the  
82 graphite in the fuel and reflector blocks, the fuel compact matrix, and the graphite found in the  
83 TRISO particles. The core comprises a hexagonal lattice of blocks, which is shown in Fig. 1. The  
84 focus of this study is on the prismatic fuel block, which is described in more detail in the  
85 remainder of this section.

86 The reference prismatic fuel block, which is shown in Fig. 2, comprises a hexagonal lattice of  
87 fuel compacts and coolant channels that are embedded in graphite. Each cylindrical fuel  
88 compact comprises TRISO fuel particles that are randomly dispersed in graphite. The fuel kernel  
89 is uranium oxycarbide ( $UC_{0.5}O_{1.5}$ ), the uranium of which is 15.5 wt.% U-235/U. The  
90 specifications of the TRISO particles are provided in Table 1, and those of the fuel compacts and  
91 fuel block are provided in Table 2, which are obtained from [12]. Three additional levels of  
92 uranium enrichment are also analyzed in this study: 5, 10, and 19.75 wt.% U-235/U.

93 The lattice physics model of the hexagonal prismatic fuel block comprises a single layer of fuel  
94 compacts, each of which is 4.928 cm in length and contains 6416 TRISO particles. In this model

95 the total power is 36 kW, which is the power per compact (172 W) multiplied by the 210 fuel  
96 compact locations per fuel block, and rounded to the nearest kW. The reference temperatures  
97 of the materials in the fuel block are based on thermal-hydraulics calculations presented in [13],  
98 the results of which are averaged and rounded to the nearest 5 K, and are shown in Table 3.  
99 The composition of  $UC_{0.5}O_{1.5}$  is identical to that of [13], and is shown in Table 4.

## 100 **2.2 PRISMATIC FUEL BLOCK WITH ANNULAR-TYPE FUEL PELLETS**

101 In a modified fuel block with annular-type fuel pellets, the fuel compacts of the reference fuel  
102 block are replaced with heterogeneous, multi-clad, annular fuel elements in which the fuel is in  
103 the form of two concentric, hollow cylinders as is shown in Fig. 3.

104 The purpose of having two annular fuel layers is for evaluating more heterogeneous fuel  
105 element design concepts, such as those with enriched uranium on the outside (in the form of  
106  $UO_2$ ,  $UCO$ ,  $UC$ , or  $UN$ ) and using a fertile material on inside, either thorium (in the form of  $ThO_2$ ,  
107  $ThCO$ ,  $ThC$ , or  $ThN$ ) or a mix of thorium and depleted uranium (DU) (in the form of  $(Th,DU)O_2$ ,  
108  $(Th,DU)CO$ ,  $(Th,DU)C$  or  $(Th,DU)N$ ).

109 A fuel element, including endcaps, extends from the bottom to the top of the 79-cm high  
110 prismatic fuel block. The lattice physics model comprises a 4.928 cm long mid-section of this  
111 element, which excludes the endcaps.

112 The materials that comprise the fuel element are listed in Table 5. The non-fuel material (i.e.,  
113 the carbon-based materials and SiC) are identical to those in the TRISO fuel of the reference  
114 concepts.

115 Table 6 lists the annular fuel element concepts that are analyzed in this study to evaluate the  
116 effects of varying fissionable materials in the fuel annuli. Three of these concepts have 100%  
117 uranium with enrichments of 5, 10, and 19.75 wt.% U-235/U, respectively. The other concepts  
118 comprise roughly equal volumes of uranium and thorium, which are either blended or in  
119 separate fuel annuli. One of these concepts includes depleted uranium blended with Th for the  
120 purpose of reducing the weight fraction of U-233 in uranium in the spent fuel, to help improve  
121 proliferation resistance. The nuclide compositions for each type of fuel are listed in Table 7.

122 Thorium is considered an attractive alternative fertile fuel, since it is abundant (nearly 3 to 4  
123 times as abundant as uranium) and can be used to complement and extend uranium resources  
124 [20]. Previous studies have shown that thorium-based fuels can help increase fuel burnup and  
125 uranium utilization, and thorium-based fuels can give more negative fuel temperature reactivity  
126 coefficients (FTRCs), which is advantageous for enhanced safety [8], [9], [10].

127 The annular fuel element contains a larger volume of fuel than that of the reference fuel  
128 compact, with the fuel element and fuel compact comprising 3.88 cm<sup>3</sup> and 0.26 cm<sup>3</sup> of fuel,  
129 respectively. The difference in fuel volume is substantial, differing by a factor of  $\sim 3.88/0.26$   
130  $\sim 14$ . The larger volume of fuel in the annular fuel element design concept permits longer fuel  
131 residence times due to reduced specific power, since the total power is the same as in the  
132 reference concept.

133 The added fuel also replaces a large quantity of graphite in the compact. This change, combined  
134 with the large increase in fuel volume, significantly reduces the ratio of carbon to fissile  
135 uranium atoms (or any fissile atoms), C/U-235, and thus significantly reduces moderation, and  
136 thus makes the neutron energy spectrum become harder, faster, and non-thermal. As a result,



137 the hardening of the neutron energy spectrum will make the fuel block sub-critical ( $k$ -effective  
138  $\leq 1.000$ ;  $k$ -infinity  $\leq 1.000$ ) due to insufficient moderation.

139 The reference fuel design for the MHTGR-350 with TRISO fuel particles has already been  
140 optimized (or nearly optimized) to achieve the C/U-235 ratio that achieves sufficient  
141 moderation to create a thermal neutron energy spectrum, and also achieves sufficiently high  
142 reactivity ( $k$ -infinity). Thus, any significant changes to the loading of fissile fuel in the prismatic  
143 fuel block is going to require other modifications to maintain a thermal neutron energy  
144 spectrum.

145 Thus, the replacement of fuel compacts with annular fuel elements also requires the  
146 replacement of several fuel elements and coolant channels with special moderator elements to  
147 improve moderation to achieve a fuel block that is super-critical in the core at the beginning of  
148 cycle (BOC). The configuration of moderator elements in the fuel block is shown in Fig. 4. This  
149 alternative configuration has 108 moderator holes on the outside, 12 moderator holes on the  
150 inside, 132 fuel holes, and 66 coolant holes. The number of fuel and coolant holes have been  
151 reduced from the original reference design (210 fuel holes, 108 coolant) holes by approximately  
152 40% ( $132/210 \sim 0.63$ ;  $66/108 \sim 0.61$ ).

153 Each moderator element comprises a cylindrical  ${}^7\text{LiH}$  pellet (0.73 cm radius) encased in SiC  
154 cladding (0.794 cm outer radius). Lithium hydride ( ${}^7\text{LiH}$ ) is chosen for the additional moderation  
155 since it is a more “efficient” moderator than carbon in graphite, with a much shorter slowing-  
156 down distance. The Li is enriched to 99.995 at.% Li-7/Li to reduce neutron capture in Li-6 nuclei.

157

158 **3. EVALUATION CRITERIA**

159 **3.1 FUEL CONSUMPTION**

160 Annual fuel consumption ( $Q_{EU}$ ) for a full SM-HTGR core is calculated for each concept using  
161 Equation (1). In a 3-batch fueling scheme, the mass of fresh fuel that is loaded into the core  
162 during refueling is 1/3 of the mass of fuel in the core, and the interval of time between  
163 refueling is 1/3 of the fuel residence time. Equations (2) and (3) are used to calculate the annual  
164 natural uranium (NU) consumption ( $Q_{NU}$ ), where  $\mathbf{R}$  is the NU feed to enriched uranium product  
165 ratio.

$$Q_{EU} = \frac{L_{EU}}{T} \quad (1)$$

$$\mathbf{R} = \frac{\mathbf{x}_p - \mathbf{x}_t}{\mathbf{x}_f - \mathbf{x}_t} \quad (2)$$

$$Q_{NU} = Q_{EU} \mathbf{R} \quad (3)$$

$L_{EU}$  is the mass of enriched uranium that is loaded into the core during refueling (i.e.,  
1/3 of the core for 3 batch refueling).

$T$  is the duration between refueling (i.e., 1/3 of the fuel residence time for 3 batch  
refueling).

$\mathbf{x}_p$  is the wt.% of U-235 in enriched uranium.

$\mathbf{x}_f$  is the wt.% of U-235 in NU, which is assumed to be 0.711 wt.% U-235/U.

$x_t$  is the wt.% of U-235 in the enrichment tails, which is assumed to be 0.2 wt.%  
U-235/U.

166 In this study there are four grades of enriched uranium that are used in the fuel concepts: 5  
167 wt.% U-235/U ( $R = 9.4$ ), 10 wt.% U-235/U ( $R = 19.2$ ), 15.5 wt.% U-235/U ( $R = 29.9$ ), and 19.75  
168 wt.% U-235/U ( $R = 38.3$ ).

### 169 **3.2 REACTIVITY COEFFICIENTS**

170 Fuel, graphite, and hydrogen moderator temperature coefficients of reactivity are calculated  
171 over a range of temperatures and burnups. For each annular fuel concept, Table 8 shows the  
172 burnups and material temperatures at which  $k_{inf}$  (infinite multiplication factor) is calculated  
173 using SERPENT 2. The same values, excluding the hydrogen-based moderator compact  
174 temperature variations, are also used for the reference TRISO fuel concepts. Within each row of  
175 Table 8, a SERPENT 2 calculation is conducted for each combination of burnup fraction (i.e., the  
176 associated fuel composition at a given burnup level) and temperature of the material in the  
177 right-most column, with the temperatures of all other materials set to their respective  
178 reference values. The  $k_{inf}$  are then used to calculate the temperature coefficients of reactivity  
179 over the range of temperatures  $[T_1, T_2] = [300 \text{ K}, 600 \text{ K}]$ ,  $[600 \text{ K}, 900 \text{ K}]$ ,  $[900 \text{ K}, 1200 \text{ K}]$ , and  $[1200$   
180  $\text{ K}, 1500 \text{ K}]$  at the indicated burnup ( $B$ ) using Equation (4).

$$C(B, T_1, T_2) = \frac{k_{inf}(B, T_1) - k_{inf}(B, T_2)}{T_1 - T_2} \quad (4)$$

181 **4. METHODS**

182 **4.1 LATTICE PHYSICS CALCULATIONS**

183 The lattice physics calculations are performed using the SERPENT 2 (version 2.1.31) Monte  
184 Carlo (MC) neutron transport and burnup/depletion code [15]. SERPENT 2 calculates the  
185 continuous energy neutron flux in two-dimensional (2D) or three-dimensional (3D) geometries  
186 using MC methods to simulate neutron histories, and it calculates the evolution of fuel  
187 composition with burnup.

188 All results presented in this document are calculated using the ENDF/B-VII.0 nuclear data library  
189 that is distributed with SERPENT 2. The results are calculated on the Minerva cluster using 550  
190 generations (or cycles), with 2 million neutrons per generation. The first 50 generations are  
191 used to achieve convergence of the criticality source calculation and are not included in the  
192 calculation of the reaction rates and output data statistics.

193 The cross-section and thermal scattering data that is used for the given material temperature  
194 are listed in Table 9. Each material temperature matches the temperature at which the  
195 corresponding cross-section data were evaluated. With respect to thermal scattering data,  
196 there is no graphite data at 300 K, 900 K, or 1500 K. Instead, the thermal scattering data  
197 evaluated at the nearest lower temperature is used at these material temperatures. The  
198 material densities in the model are not modified in these calculations.

199 No thermal scattering data is used for the LiH moderator compacts due to there being no such  
200 data for Li-bound hydrogen.

201 **4.2 CALCULATION OF K-EFFECTIVE**

202 All SERPENT calculations of the lattice physics model of a single prismatic fuel block are  
 203 conducted using reflective boundary conditions on a fuel block. To calculate the effective  
 204 neutron multiplication factor (k-effective, or  $k_{\text{eff}}$ ) considering expected neutron leakage in a full,  
 205 finite-sized reactor core, a 2-group diffusion leakage model with homogenized cross-sections  
 206 generated by SERPENT 2 is used along with a user-defined geometric buckling value associated  
 207 with the full finite core geometry. The formula for calculating  $k_{\text{eff}}$  is given in Equation (5). This  
 208 calculation provides an approximate value of  $k_{\text{eff}}$  for comparison purposes in this study. A more  
 209 accurate value of  $k_{\text{eff}}$  will be calculated using a full core physics model with SERPENT (or a  
 210 deterministic core physics code) in future work.

$$k_{\text{eff}} = \frac{\nu\Sigma_{f1} + \nu\Sigma_{f2} \frac{\Sigma_{S(1\rightarrow2)}}{(D_2B^2 + \Sigma_{R2})}}{(D_1B^2 + \Sigma_{R1}) - \Sigma_{S(2\rightarrow1)} \frac{\Sigma_{S(1\rightarrow2)}}{(D_2B^2 + \Sigma_{R2})}} \quad (5)$$

$B^2$  is the geometric buckling, assuming  $B_1^2 = B_2^2$ .

$\nu\Sigma_{fn}$  is the fission neutron production cross-section for group  $n$ .

$\Sigma_{S(n\rightarrow m)}$  is the neutron scattering cross-section from group  $n$  to  $m$ .

$D_n$  is the diffusion coefficient for group  $n$ .

$\Sigma_{Rn}$  is the removal cross-section for group  $n$ .

211 The value of  $B^2$  is calculated using Equation (6), assuming a cylindrical, homogeneous core with  
 212 active height ( $H_a$ ) of 793 cm [11] and an effective radius ( $R_a$ ) of 153.5 cm. The effective radius is

213 approximated based on the horizontal area of 66 fuel blocks, which are shown in Fig. 1. Each  
214 fuel block is hexagonal with a flat-to-flat length of 36 cm (Fig. 2), and thus is 1122.4 cm<sup>2</sup> in area.  
215 A circle with an area of 1122.4 x 66 = 74,076.3 cm<sup>2</sup> has an effective radius of 153.5 cm. Thus,  
216 the geometric buckling is calculated to be 2.61E-4 cm<sup>-2</sup>. This value of geometric buckling  
217 neglects the effect of the inner and outer graphite reflectors in reducing neutron leakage, thus  
218 it is likely an overestimate of the neutron leakage.

$$B^2 = \left(\frac{2.405}{R_a}\right)^2 + \left(\frac{\pi}{H_a}\right)^2 \quad (6)$$

219  
220 The use of SERPENT for performing lattice physics calculations, and then imposing a geometric  
221 buckling that is based on the bare cylindrical core dimensions, with zero extrapolation distance,  
222 and using a diffusion-based leakage model to estimate the core  $k_{\text{eff}}$  is considered a conservative  
223 approximation, in that it will over-estimate leakage, and under-estimate exit burnup. In a full-  
224 core SERPENT model, with the presence of radial and axial reflectors, the core leakage will be  
225 reduced. For the purpose of carrying out initial scoping and exploratory calculations to  
226 evaluate fuel behavior, exit burnup, reactivity coefficients, and other performance and safety  
227 characteristics, this more simplified and approximate approach using lattice physics calculations  
228 is considered both practical and satisfactory. The results from these lattice physics calculations  
229 and their extrapolation to full-core behavior are a pre-cursor to performing more detailed full-  
230 core analyses with complete modeling of both radial and axial reflectors.

231

232 **4.3 EXIT BURNUP**

233 The single-batch exit burnup and fuel residence time correspond to the burnup step in which  
234  $k_{\text{eff}} = 1.0$ . A two-point linear interpolation is used to estimate the burnup and fuel residence  
235 time that correspond to  $k_{\text{eff}} = 1.0$  using the values of  $k_{\text{eff}}$ , burnup, and fuel residence time at the  
236 last burnup step where  $k_{\text{eff}} > 1.0$  and at the first burnup step where  $k_{\text{eff}} < 1.0$ . In this study a 3-  
237 batch refueling scheme is used, which is also used in previous studies of the MHTGR-350 [12]  
238 [15]. The linear reactivity model is used to estimate the exit burnup and fuel residence time for  
239 a 3-batch refueling scheme, which is  $3/2$  times the single-batch exit burnup and fuel residence  
240 time, respectively. The formula for the linear reactivity model is:  $BU(n) = BU(1) \times 2n/(n+1)$ . For a  
241 3 batch scheme,  $n = 3$ , and  $BU(3) = BU(1) * 6/4 = 1.5 * BU(1)$ .

242

243 **4.4 ESTIMATED FULL CORE FUEL MASS**

244 The fuel and NU consumption in this study are calculated from the mass of fuel in a core. The  
245 total mass of fuel in the core is calculated based on a description of the MHTGR-350 from [11],  
246 which describes the two types of fuel blocks in the core: a standard block and a reserve  
247 shutdown control (RSC) block, which are referred to as “fuel elements” in that document. The  
248 RSC block has fewer fuel holes than the standard block in order to make room for control  
249 devices. In total, there are 660 prismatic fuel blocks in the MHTGR-350 core. There are 540 (54  
250 fuel columns × 10 blocks per column) standard and 120 (12 fuel columns × 10 blocks per  
251 column) RSC blocks in the core, each of which has 210 and 186 fuel holes, respectively, in the  
252 reference MHTGR-350 design. Each fuel hole contains 15 fuel compacts in a 79-cm high  
253 prismatic fuel block. Thus, there are  $15 \times (210 \times 540 + 186 \times 120) = 2,035,800$  fuel compacts in the  
254 reference core. Each fuel compact comprises 6416 TRISO particles, which is 2.5 gU/compact. As  
255 such, the reference core contains 5,086 kgU.

256 Due to the replacement of some fuel compacts with moderator compacts in the annular fuel  
257 block, there are 156 and 134 fuel holes per standard and RSC block, respectively. Thus, there  
258 are a total of  $156 \times 540 + 134 \times 120 = 100,320$  annular fuel elements in the core. The length of  
259 an annular fuel element is 73.92 cm, thus, there is  $29.1 \text{ cm}^3$  of fuel in each of the inner and  
260 outer annuli of a fuel element. Given the make-up of each annular fuel concept in Table 6 and  
261 the composition of each fissionable material in Table 7, the total mass of fuel in a core for each  
262 annular fuel concept is listed in Table 10.



263 **5. RESULTS**

264 **5.1 REFERENCE VERSUS BENCHMARK CALCULATIONS**

265 The calculated value of  $k_{inf}$  versus burnup for the benchmark MHTGR-350 model and the  
266 reference model developed for this study are shown in Fig. 5. The data for the benchmark case  
267 is taken from [13]. The values of  $k_{inf}$  calculated using the reference model in this study are very  
268 similar to those from the benchmark calculations, with a difference of 3.6 mk at 0 burnup and a  
269 maximum difference of 8.0 mk, which occurs at 100 MWd/kgHM.

270 **5.2 ANNULAR VERSUS REFERENCE FUEL BLOCK**

271 In this section the reference fuel concepts R5, R10, and R19.75 with 5, 10, and 19.75 wt.% U-  
272 235/U, respectively are compared with the annular fuel concepts A5, A10, and A19.75.

273 **5.2.1 NEUTRON ENERGY SPECTRUM**

274 The differences between the reference and annular fuel blocks affect the neutron energy  
275 spectra. The plot in Fig. 6 shows that the annular concepts have a lower proportion of neutron  
276 flux in the epithermal range, between  $10^{-6}$  MeV and 0.1 MeV, which is due to their reliance  
277 on LiH as the primary moderator. Neutrons require fewer interactions with hydrogen in order  
278 to be slowed down to thermal energies than with carbon, thus neutrons reach thermal energies  
279 in much less time. This figure also shows that the annular concepts have higher neutron flux in  
280 the fast range, above 0.1 MeV, which is due to their larger volume and mass of fissionable  
281 material. Unlike the epithermal and fast energy ranges, the differences in thermal neutron flux  
282 between the reference and annular fuels vary substantially with enrichment. As shown in Fig.  
283 6, as the fissile content is increased, the ratio of C/U-235 and H/U-235 are decreased, making

284 the neutron energy spectrum harder, which is true for both reference and annular-type fuels.  
285 However, due to the more heterogeneous design and arrangement of moderator rods in the  
286 annular-type design, which experiences neutron moderation due to hydrogen, graphite, and to  
287 a lesser degree, lithium, there is a shift in the thermal flux between low-enrichment (5 wt% U-  
288 235/HM) and high enrichment (19.75 wt% U-235/U) fuel.

289 For example, the thermal flux for R5 is much higher than that of A5 but the thermal flux of  
290 A19.75 is higher than that of R19.75. The data shown appears to indicate that the reference  
291 fuel concepts are somewhat under-moderated, and so when the U-235 content is doubled from  
292 5 wt% U-235/U to 10 wt% U-235/U, the thermal neutron flux drops significantly, and when the  
293 fissile content is doubled again to 19.75 wt% U-235/U, the spectrum in the TRISO fuel becomes  
294 harder still. In contrast, it appears that the fuel block with annular-type fuel elements and LiH  
295 moderator rods may actually be slightly over-moderated, since it experiences smaller changes  
296 in the thermal neutron flux when the fissile content is doubled from 5 wt% U-235/U to 10 wt%  
297 U-235/U.

### 298 **5.2.2 NEUTRON MULTIPLICATION FACTOR**

299 For each level of uranium enrichment, the infinite neutron multiplication factor ( $k_{inf}$ ) is over 90  
300 mk higher for the annular fuel at 0 burnup, as is shown in Fig. 8. These higher values are due to  
301 the higher concentration of U-235 in the annular fuel which leads to a greater influence of the  
302 spatial self-shielding effect. Neutron leakage in the annular fuel is reduced by over 90 mk,  
303 shown in Fig. 8, due to the addition of LiH moderator compacts on the periphery of the fuel  
304 block. The increased  $k_{inf}$  and reduced leakage combine to increase the effective multiplication  
305 factor ( $k_{eff}$ ) by over 200 mk, which is shown in Fig. 9.

306 The higher values of  $k_{\text{eff}}$  lead to higher exit burnups for each of the annular fuel concepts  
307 relative to the reference concept with the same initial uranium enrichment, as shown in Fig. 10.  
308 Due to this higher exit burnup and the larger mass of uranium in the annular fuel concepts, the  
309 fuel residence times for the annular concepts are all over 20 years longer than those of the  
310 reference fuel. Note that such long residence times may not be feasible due to limits on the fast  
311 neutron fluence that graphite can experience before having to be removed from the core. Due  
312 to its higher burnup, using the annular fuel reduces the annual NU consumption (Fig. 12) by  
313 between 48 and 72%, where the reduction is highest for 5 wt.% U-235/U and lowest for 19.75  
314 wt.% U235/U. The lowest NU consumption is achieved using 10 wt.% U-235/U, which is 4% less  
315 than using 5 wt.% U-235/U: the annular concept with the highest NU consumption.

### 316 **5.2.3 REACTIVITY COEFFICIENTS**

317 An apparent tradeoff of using the current annular fuel concepts is the resulting increase in  
318 temperature reactivity coefficients. The plot in Fig. 13 shows that the average of the FTTCs over  
319 burnup and temperature are as much as 0.064 mk/K higher, although still negative at all  
320 temperatures and burnups. The average graphite temperature reactivity coefficients (GTRCs)  
321 are also higher by as much as 0.015 mk/K, as shown in Fig. 14, and are slightly positive, ranging  
322 between +0.002 mk/K and +0.004 mk/K. Although conventional HTGR fuel designs with TRISO  
323 fuel particles and graphite moderator have a negative GTRC, the annular fuel design concept in  
324 this study, combined with the use of a hydrogen-based moderator leads to the slightly positive  
325 GTRC. For comparison, other HTGR-type reactors with alternative coolants and moderators,  
326 such as the SmaHTR, a molten FLiBE-cooled reactor, have also demonstrated slightly positive  
327 GTRC values, ranging from +0.0002 mk/K to +0.0011 mk/K [17].

328

329

330 Since the GTRCs are smaller in magnitude than the FTRCs, which means that the core  
331 temperature coefficient of power would likely be negative but for the positive ( $\sim 0.090$  mk/K)  
332 hydrogen temperature reactivity coefficients (HTRCs) shown in Table 11. This result concurs  
333 with other studies of alternative moderators, which have also found that hydrogen-based  
334 moderators have positive reactivity coefficients [16]. These results are attributed to the  
335 reduced neutron absorption in hydrogen with increasing temperature, along with slight  
336 changes in the neutron energy spectrum which will lead to reduced neutron absorption in U-  
337 235, U-238 and other actinides.

338 However, the present evaluation of HTRCs does not consider the effects of density changes in  
339 solid LiH with temperature. Given that the density of solid LiH decreases with temperature by  
340 between  $1.1 \times 10^{-4}$  and  $1.4 \times 10^{-4}$  g/cm<sup>3</sup>/K [18], as illustrated in Fig. 16, it is expected that the  
341 calculated HTRC would still be quite positive if the density changes were considered for solid  
342 LiH, but would become much less positive, or perhaps even negative for temperatures beyond  
343 its melting point of 692°C / 965 K [5], [18]. In this concept it is assumed that each LiH rod  
344 extends the full height of the core, and that there is space at the axial ends of each moderator  
345 compact to allow for thermal expansion. It is also noted that the LiH moderator rods will be at  
346 a temperature between that of the helium coolant (750 K) and the graphite block (835 K), (see  
347 Table 3) which is well below the melting point of LiH ( $\sim 965$  K).

348 Since the HTRC decreases with increasing mass of U-235 in the fuel, it is expected that reducing  
349 the volume of LiH moderator in the core, and hence further reducing the H/U-235 ratio, would  
350 further reduce the HTRC, although it will have an impact on the exit burnup and NU  
351 consumption. Reducing the H/U-235 ratio can be achieved simply by removing  ${}^7\text{LiH}$  moderator  
352 rods, and replacing them with fuel rods.

353

354

355 **5.3 ANNULAR FUEL BLOCK: URANIUM VERSUS URANIUM-THORIUM FUEL**

356 In this section the uranium and uranium-thorium annular fuel concepts are compared. The  
357 uranium fuel with 5 wt.% U-235/U (A5) is compared with the heterogeneous uranium-thorium  
358 fuel concept (U10|Th) that is 50 vol.% uranium (10 wt.% U-235/U), both of which have fissile  
359 content of ~5 wt.% U-235/HM. The other uranium-thorium concepts, U19.75+Th and  
360 U19.75|DU+Th, are 50 vol.% uranium that is 19.75 wt.% U235/U, for a fissile content of ~10  
361 wt.% U-235/HM. Thus they are compared with A10, which has 10 wt.% U-235/HM. Since Th in  
362 ThCO is 11% less dense than U in UCO, the thorium-uranium concepts have 6% less mass of HM  
363 than the uranium concepts.

364 The plot in Fig. 15 shows that replacing 50 vol.% of the uranium with thorium reduces  $k_{eff}$  for  
365 fresh fuel due to neutron absorption in Th and slows the decline in  $k_{eff}$  with burnup due to U233  
366 build-up. These effects influence the exit burnup, fuel residence time, and NU consumption,  
367 which are shown in Table 12. The difference in  $k_{eff}$  for fresh fuel between the uranium and  
368 uranium-thorium fuels is largest (83 mk) for the 5% fissile fuel concepts A5 and U10|Th. The  
369 U10|Th fuel has 2% lower exit burnup, which indicates that U-233 is not being bred quickly  
370 enough to compensate for the initial drop in  $k_{eff}$  before the fuel block becomes subcritical. This  
371 concept also has a 8% shorter fuel residence time, which is a consequence of its lower burnup  
372 and lower mass of HM. This reduction in residence time, and the more than 2 times higher NU  
373 feed to product ratio ( $R$ ) for the uranium in U10|Th (10 wt.% U-235/U) than that of uranium in  
374 A5 (5 wt.% U-235/U), combine to increase NU consumption by 11%.

375 The differences in  $k_{\text{eff}}$  between the 10% fissile uranium and uranium-thorium concepts for fresh  
376 fuel are 59, 66, and 57 mk, for U19.75|Th, U19.75+Th, and U19.75|DU+Th, respectively. The  
377 exit burnup of each of these concepts is ~5% higher than that of A10, but the NU consumption  
378 of each concept is also slightly (< 1%) higher than that of A10. This increased NU consumption is  
379 due to the 0.6 to 0.7% reduction in fuel residence time, which more than offsets the 0.2% lower  
380 NU feed required to produce enriched uranium for a uranium-thorium fuel block.

381 For the heterogeneous and homogenous fuel concepts, U19.75|Th and U19.75+Th,  
382 respectively, the differences in exit burnup, fuel residence time, and NU consumption are small.  
383 The homogeneous concept has 0.2% higher exit burnup and fuel residence time, and 0.2%  
384 lower NU consumption, which indicates that the homogeneous fuel results in more breeding of  
385 U-233 than that of the heterogeneous fuels.

386 The replacement of 10 vol.% of the Th in the inner annulus of the U19.75|Th concept with DU  
387 causes a 2 mk increase in  $k_{\text{eff}}$  at 0 burnup, a 0.6% reduction in exit burnup, and negligible  
388 differences in fuel residence time and NU consumption.

389 Replacing half of the uranium with thorium in the annular fuel concepts causes a reduction in  
390 the average fuel, graphite, and hydrogen temperature reactivity coefficients, as is shown in  
391 Table 13. The FTRCs of the uranium-thorium fuel concepts are all more than 0.005 mk/K less  
392 than those of the uranium-only fuel concepts due to the greater increase in Th-232 capture  
393 cross-section with temperature relative to that of U-238, which was also observed in [19].

394 There is also a reduction of 0.005 mk/K, or more, in the HTRCs. The reduction in GTRCs is  
395 0.001 mk/K.

396 **6. SUMMARY AND CONCLUSIONS**

397 SERPENT lattice physics calculations have been carried out to evaluate the performance and  
398 safety characteristics of a modified HTGR prismatic fuel block concept, based on the MHTGR-  
399 350 benchmark problem. The key changes were to replace the conventional TRISO-filled fuel  
400 compacts with heterogeneous, multi-layer annular fuel pellets made with UCO, ThCO,  
401 (U,Th)CO, or (DU,Th)CO. These fuel pellets have multiple protective cladding layers of pyrolytic  
402 carbon (PyC) and silicon carbide (SiC), which is anticipated to give it robust qualities similar to  
403 TRISO particles, but at a more macroscopic scale. With the increased loading of uranium in the  
404 fuel block, it was necessary to replace up to 78 fuel holes and 42 coolant holes (120 holes total)  
405 with a hydrogen-based moderator ( $^7\text{LiH}$ ), in order to ensure a thermal neutron energy spectrum  
406 in the lattice.

407 Results demonstrate that the modified fuel concept has several advantages and challenges  
408 relative to the conventional MHTGR-350 design concept. With the increased uranium loading  
409 (almost by a factor of 10), and the reduced neutron leakage (by 60 mk or more) due to the use  
410 of a hydrogen-based moderator ( $^7\text{LiH}$ ), much higher burnup levels and lower natural uranium  
411 consumption levels can be achieved with the same level of uranium enrichment. For example,  
412 the annular-type fuel pellets made with UCO with 19.75 wt.% U-235/U can achieve nearly  
413 double the burnup ( $\sim 201$  MWd/kgU), as TRISO-loaded fuel compacts ( $\sim 105$  MWd/kg).

414 Estimated uranium consumption in a full reactor core is reduced from  $\sim 46.5$  tonnes-NU/year  
415 for the TRISO-based fuel down to  $\sim 24.0$  tonnes-NU/year for the annular-type fuel. In addition,  
416 the expected fuel lifetime / residence time in a HTGR core before the fuel must be replaced is  
417 increased dramatically, to values as high as 76.6 years (with 3-batch refuelling) for annular –



418 type fuel made with 19.75 wt.% U-235/U in the form of UCO. By comparison, fuel blocks with  
419 TRISO-type fuel in compacts will need to be replaced after ~4.2 years. Hence, the modified fuel  
420 design could be very attractive for developing HTGR-SMRs as “nuclear batteries” that are  
421 fuelled only once, although this may be limited due to irradiation damage to various materials  
422 in the core, including the fuel, moderator, graphite, and other components.

423 The use of thorium as a fertile material in either homogeneous annular fuel pellets ((U,Th)CO in  
424 outer and inner fuel annuli), or heterogeneous annular fuel pellets (UCO in outer fuel annulus,  
425 ThCO or (Th,DU)CO in inner fuel annulus) gives a comparable or slightly higher burnup than  
426 UCO fuels with the same average fissile content (wt.% U-235/HM). The residence time is slightly  
427 smaller for thorium-based fuels, due to the lower density of ThCO relative to UCO. The annual  
428 NU consumption rate for thorium-based fuels is slightly higher (up to 10%) in comparison with  
429 UCO fuels with the same average fissile content, although at a high fissile content level (~10  
430 wt.% U-235/(U+Th), there is essentially no difference between the UCO and the (U,Th)CO fuels.

431 The challenge of the current design concept of the modified HTGR fuel concept with annular-  
432 type fuels, and <sup>7</sup>LiH moderator rods, is that in comparison to the conventional MHTGR-350  
433 design with TRISO-based fuel compacts, it has less negative fuel temperature reactivity  
434 coefficients, FTRC, (as small as -0.028 mk/K), and slightly positive graphite and hydrogen  
435 moderator temperature coefficients, with values as high as +0.015 mk/k (for graphite MTC) and  
436 +0.19 mk/K (for hydrogen MTC). Thorium-based annular fuels made with (U,Th)CO appear to  
437 have more negative FTCs, and less positive graphite and hydrogen temperature coefficients  
438 relative to annular fuels made with UCO, which is advantageous from a reactor safety  
439 perspective.

440 It is speculated that the current concept is “*over-moderated*”, and the number of  ${}^7\text{LiH}$  rods need  
441 to be reduced. Although full-core physics calculations would need to be performed to better  
442 quantify and assess the resulting power coefficient of reactivity (PCR), it is anticipated that the  
443 PCR could be too high, and an active control system would be required to prevent a power  
444 transient. Thus, further modifications to the design concept will be required to ensure smaller  
445 or negative moderator temperature coefficients and a negative PCR.

446

447 **7. OPTIONS FOR FUTURE WORK AND IMPROVEMENTS**

448 Based on what has been learned from the current studies of uranium and uranium-thorium  
449 oxy-carbide fuels in modified prismatic HTGR fuel blocks with annular-type fuel pellets (instead  
450 of conventional TRISO-based fuel compacts) and  $^7\text{LiH}$  moderator fuel rods, the following are  
451 potential options for future work:

- 452 • Evaluate the effects of using graphite thermal scattering libraries at more appropriate  
453 temperatures on the lattice physics calculations.
- 454 • Evaluate alternative fuel matrix materials, including oxides, nitrides, and carbides.
- 455 • Evaluate plutonium/thorium fuels in the form of oxides, nitrides, carbides, and oxy-  
456 carbides. The plutonium isotopic composition could be based on either spent LEU fuel  
457 from a pressurized water reactor (PWR) fuel or spent NU fuel from a pressure tube  
458 heavy water reactor (PT-HWR).
- 459 • Evaluate alternative materials for moderator rods, including  $^7\text{LiD}$ ,  $^7\text{LiOH}$ , and NaOH.  
460 Hydroxides are potentially advantageous over hydrides, since they can operate at much  
461 higher temperatures before boiling or undergoing decomposition. For example, NaOH  
462 boils at 1,388 °C, well above the expected maximum operating temperature of an HTGR.  
463 Recent studies have shown that hydroxides could be an attractive moderator material  
464 for compact SMRs [21].
- 465 • Adjust the number of  $^7\text{LiH}$  moderator rods to a lower number to potentially reduce the  
466 hydrogen moderator temperature coefficient, such that the modified HTGR lattice will  
467 have a negative power coefficient of reactivity.

- 468       • Account for changes in the  ${}^7\text{LiH}$  density with temperature, and implement thermal  
469       scattering data appropriate for H bound in a hydride. Current calculations did not  
470       account for such effects, which will have some impact on the evaluation of  $k_{\text{inf}}$ ,  $k_{\text{eff}}$  and  
471       reactivity coefficients.
- 472       • Carry out full-core physics calculations of an HTGR core with a number of selected  
473       annular-type fuel concepts to get a better estimate of the power distributions and the  
474       exit burnup of the fuel. Full core modeling will provide a better estimate of the effects  
475       of radial and axial reflectors, neutron leakage, and the effect of control rods used for  
476       excess reactivity control and adjusting power distributions.
- 477       • Carry out thermal-hydraulic and heat transfer calculations to obtain better estimates of  
478       the temperature distributions in the fuel and moderator with annular-type fuel pellets  
479       and hydrogen-based moderator rods ( ${}^7\text{LiH}$ ).
- 480       • Evaluate the performance of the annular fuel with respect to fission product retention.
- 481       • Investigate the replacement of fuel block graphite with materials that are more resistant  
482       to radiation damage.
- 483

484

485 **ACKNOWLEDGMENTS**

486 The authors would like to thank Gerhard Strydom, Rike Bostelmann, Pascal Rouxelin, and Nick  
487 Brown for sharing their expertise on HTGRs.

488 The authors also recognize the oversight, help, and assistance provided by the following staff at  
489 Canadian Nuclear Laboratories (CNL): Rosaura Ham-Su, Ali Siddiqui, Ashlea V. Colton, Sam Kelly,  
490 Huiping V. Yan, Peter Pfeiffer, Jonathan McKay, and Tina Wilson.

491 **FUNDING**

492 This work is funded by Atomic Energy of Canada Limited (AECL), under the auspices of the  
493 Federal Nuclear Science and Technology (FST) Program.

494

495 **NOMENCLATURE**

496

$D_n$	diffusion coefficient for group $n$ , m
$B^2$	geometric buckling for a core; $\left(\left(\frac{2.405}{R_a}\right)^2 + \left(\frac{\pi}{H_a}\right)^2\right)$ , $m^{-2}$
$BU(n)$	exit burnup for $n$ batch refueling, MWd/kg
$C(B, T_1, T_2)$	temperature coefficient of reactivity at burnup $B$ , between temperatures $T_1$ and $T_2$ ; $\left(\frac{k_{inf}(B, T_1) - k_{inf}(B, T_2)}{T_1 - T_2}\right)$ , mk/K
$H_a$	effective height of the cylindrical core, m
$L_{EU}$	mass of enriched uranium that is loaded into the core during refueling, kg
$mk$	unit for the difference between two values of neutron multiplication factors; $(10^{-3} \Delta k)$
$MWd$	derived unit of energy; $(10^6 \cdot 24 \cdot 3600)$ , J
$Q_{EU}$	annual fuel consumption; $\left(\frac{L_{EU}}{T}\right)$ , kg/y
$Q_{NU}$	annual natural uranium consumption; $(Q_{EU}R)$ , kg/y
$R_a$	effective radius of the cylindrical core, m
$T$	duration between refueling, s
$y$	derived unit of time; $(3600 \cdot 24 \cdot 365)$ , s

497

498 **Greek Letters**

$\Sigma_{Rn}$	removal cross-section for group $n$ , $m^{-1}$
$\Sigma_{S(n \rightarrow m)}$	neutron scattering cross-section from group $n$ to $m$ , $m^{-1}$
$\nu \Sigma_{fn}$	fission neutron production cross-section for group $n$ , $n/m$

499

500

501 **Non-Dimensional Numbers**

$k_{eff}$	Neutron multiplication factor for a finite core; $\left(\frac{\nu \Sigma_{f1} + \nu \Sigma_{f2} \frac{\Sigma_{S(1 \rightarrow 2)}}{(D_2 B^2 + \Sigma_{R2})}}{(D_1 B^2 + \Sigma_{R1}) - \Sigma_{S(2 \rightarrow 1)} \frac{\Sigma_{S(1 \rightarrow 2)}}{(D_2 B^2 + \Sigma_{R2})}}\right)$
$k_{inf}$	Neutron multiplication factor on an infinite lattice
$R$	Ratio of natural uranium feed to enriched uranium product; $\left(\frac{x_p - x_t}{x_f - x_t}\right)$
$x_f$	weight % U-235/U in natural uranium feed
$x_p$	weight % U-235/U in enriched uranium product
$x_t$	weight % U-235/U in depleted uranium tails

502

503 **Subscripts or Superscripts**

EU	enriched uranium
----	------------------

NU	natural uranium
eff	effective
inf	infinite
f	feed or fission
p	product
t	tails

504

505 **Acronyms and abbreviations widely used in text and list of references**

2D	Two dimensional
3D	Three dimensional
BOC	Beginning of Cycle
DU	Depleted Uranium
FP	Fission Products
FTRC	Fuel Temperature Reactivity Coefficient
GTRC	Graphite Temperature Reactivity Coefficient
HM	Heavy Metal
MC	Monte Carlo
NU	Natural Uranium
PT-HWR	Pressure Tube Heavy Water Reactor
PWR	Pressurized Water Reactor
RSC	Reserve Shutdown Control
SM-HTGR	Small Modular High Temperature Gas-cooled Reactor
TRISO	Tri-Structural ISOtropic
wt.%	weight percent

506

507

508 **8. REFERENCES**

509

510 [1] World Nuclear Association, 2021, "Small Nuclear Power Reactors", [https://www.world-](https://www.world-nuclear.org/information-library/nuclear-fuel-cycle/nuclear-power-reactors/small-nuclear-power-reactors.aspx)  
511 [nuclear.org/information-library/nuclear-fuel-cycle/nuclear-power-reactors/small-](https://www.world-nuclear.org/information-library/nuclear-fuel-cycle/nuclear-power-reactors/small-nuclear-power-reactors.aspx)  
512 [nuclear-power-reactors.aspx](https://www.world-nuclear.org/information-library/nuclear-fuel-cycle/nuclear-power-reactors/small-nuclear-power-reactors.aspx).

513

514 [2] Wojtaszek, D., 2017, Potential Off-Grid Markets for SMRs in Canada, CNL Nuclear  
515 Review, Vol. 8, No. 2, 10 pages. Free download from:  
516 <https://pubs.cnl.ca/doi/10.12943/CNR.2017.00007>.

517

518 [3] Advances in Small Modular Reactor Technology Developments, A Supplement to: IAEA  
519 Advanced Reactors Information System (ARIS), International Atomic Energy Agency,  
520 2020. Free download from: [https://aris.iaea.org/Publications/SMR\\_Book\\_2020.pdf](https://aris.iaea.org/Publications/SMR_Book_2020.pdf)

521

522 [4] [https://nuclearsafety.gc.ca/eng/reactors/power-plants/pre-licensing-vendor-design-](https://nuclearsafety.gc.ca/eng/reactors/power-plants/pre-licensing-vendor-design-review/)  
523 [review/](https://nuclearsafety.gc.ca/eng/reactors/power-plants/pre-licensing-vendor-design-review/); Accessed March 01 2021.

524

525 [5] Mughabghab, S., Schmidt, S.E., and Ludewig, H., 1993, Generation of Neutronic Thermal  
526 Data in Support of Space Nuclear Propulsion, AIP Conference Proceedings 271, 965,  
527 Albuquerque, New Mexico, USA. Free download from:  
528 <https://aip.scitation.org/doi/pdf/10.1063/1.43122>

529

530 [6] Lee, H.C., Lim, H.S., and Han, T.Y., 2014, A Neutronic Feasibility Study on a Small LEU  
531 Fueled Reactor for Space Applications, Transactions of the Korean Nuclear Society  
532 Autumn Meeting, Pyeongchang, Korea, 2014. OSTI ID: 22355450

533

534 [7] Shropshire, D.E., and Herring, J.S., 2004, Fuel-Cycle and Nuclear Material Disposition  
535 Issues Associated with High-Temperature Gas Reactors, Proceedings of the Americas  
536 Nuclear Energy Symposium (ANES 2004), Miami Beach, USA. Free download from:  
537 <https://digital.library.unt.edu/ark:/67531/metadc782524/>

538

539 [8] Colton, A.V. and Bromley, B.P., 2018, Simulations of Pressure-Tube–Heavy-Water  
540 Reactor Cores Fueled with Thorium-Based Mixed-Oxide Fuels, Nuclear Technology, Vol.  
541 203, No. 2, 27 pages. Free download from:  
542 <https://www.tandfonline.com/doi/full/10.1080/00295450.2018.1444898>

543

544 [9] Colton, A.V. and Bromley, B.P., 2018, Lattice Physics Evaluation of 35-Element Mixed  
545 Oxide Thorium-Based Fuels for Use in Pressure Tube Heavy Water Reactors, Annals of



- 546 Nuclear Energy, Vol. 117, 18 pages. Free download from:  
547 <https://www.sciencedirect.com/science/article/pii/S0306454918301233>  
548
- 549 [10] Bromley, B.P., 2014, High Utilization Lattices for Thorium-Based Fuel Cycles in Heavy  
550 Water Reactors, ANS Nuclear Technology Journal, Vol. 186, No. 1, 16 pages. Free  
551 download from: <https://www.tandfonline.com/doi/abs/10.13182/NT13-86>  
552
- 553 [11] Gougar, H., Ortensi, J., Pope, M.A., Sen, S., Strydom, G., Seker, V., Collins, B., Downar,  
554 T., Baxter, A., Ellis, C., Vierow, K., Klein, A., Ivanov, K., 2012, “Prismatic Coupled  
555 Neutronics/Thermal Fluids Transient Benchmark of the MHTGR-350 MW Core Design:  
556 Benchmark Definition”, Idaho National Laboratory. Free download from:  
557 <https://art.inl.gov/NGNP/Water%20Ingress%20Assessment%20Review%20Material/INL%20Published%20Material/Preliminary%20Prismatic%20Coupled%20Neutronics%20Thermal%20Fluids%20Transient%20Benchmark%20of%20the%20MHTGR-350%20MW%20Core%20Design%2012-06-10.pdf>  
558  
559  
560  
561
- 562 [12] Pope, M.A., 2012, Transmutation Analysis of Enriched Uranium and Deep Burn High  
563 Temperature Reactors, INL/EXT-12-26423, FCR&D-FCO-2012-000149, Idaho National  
564 Laboratory Document. Free download from: [https://www.osti.gov/biblio/1056011-  
565 transmutation-analysis-enriched-uranium-deep-burn-high-temperature-reactors](https://www.osti.gov/biblio/1056011-transmutation-analysis-enriched-uranium-deep-burn-high-temperature-reactors)  
566
- 567 [13] Bostelmann, Strydom, G., and Yoon, S.J., 2015, Results for Phase I of the IAEA  
568 Coordinated Research Program on HTGR Uncertainties, Idaho National Laboratory  
569 Report INL/EXT-14-32944. Free download from:  
570 <https://inldigitallibrary.inl.gov/sites/sti/sti/6339786.pdf>  
571
- 572 [14] McMurray, J.W., Lindemer, T.B., Brown, N.R., Reif, T.J., Morris, R.N., et al., 2017,  
573 Determining the Minimum Required Uranium Carbide Content for HTGR UCO Fuel  
574 Kernels, Annals of Nuclear Energy, Vol. 104, 16 pages. Free download from:  
575 <https://www.sciencedirect.com/science/article/pii/S0306454917300567>  
576
- 577 [15] Leppänen, J., Pusa, M., Viitanen, T., Valtavirta, V., and Kaltiaisenaho, T., 2015, The  
578 Serpent Monte Carlo code: Status, Development and Applications in 2013. Annals of  
579 Nuclear Energy, Vol. 82, 9 pages. Free download from:  
580 <https://www.sciencedirect.com/science/article/pii/S0306454914004095>  
581
- 582 [16] Duchnowski, E.M., Kile, R.F., Snead, L.L., Trelewicz, J.R., and Brown, N.R., 2020, Reactor  
583 Performance and Safety Characteristics of Two-Phase Composite Moderator Concepts  
584 for Modular High Temperature Gas Cooled Reactors, Nuclear Engineering and Design,  
585 Vol. 368, paper # 110824. Free download from:  
586 <https://www.sciencedirect.com/science/article/pii/S0029549320303186>

587

588 [17] S. R. Greene, S.R., Gehin, J.C., Holcomb, D.E., Carbajo, J.J., Ilas, D., Cisneros, A.T., Pre-  
589 Conceptual Design of a Fluoride-Salt-Cooled Small Modular Advanced High-Temperature  
590 Reactor (SmAHTR), Report ORNL/TM-2010/199, Oak Ridge National Laboratory,  
591 December, 2020. Free download from: [https://www.osti.gov/biblio/1008830-pre-](https://www.osti.gov/biblio/1008830-pre-conceptual-design-fluoride-salt-cooled-small-modular-advanced-high-temperature-reactor-smahtr)  
592 [conceptual-design-fluoride-salt-cooled-small-modular-advanced-high-temperature-](https://www.osti.gov/biblio/1008830-pre-conceptual-design-fluoride-salt-cooled-small-modular-advanced-high-temperature-reactor-smahtr)  
593 [reactor-smahtr](https://www.osti.gov/biblio/1008830-pre-conceptual-design-fluoride-salt-cooled-small-modular-advanced-high-temperature-reactor-smahtr)

594

595 [18] Smith, R.L., and Miser, J.W., 1972, Compilation of the Properties of Lithium Hydride,  
596 Technical Memorandum X-483, Lewis Research Center, Cleveland, Ohio. Free download  
597 from: <https://ntrs.nasa.gov/citations/19720066808>

598

599 [19] Dobuchi, N., Takeda, S., and Kitada, T., 2016, Study on the Relation Between Doppler  
600 Reactivity Coefficient and Resonance Integrals of Thorium and Uranium in PWR Fuels,  
601 Annals of Nuclear energy, Vol. 90, 4 pages. Free download from:  
602 <https://www.sciencedirect.com/science/article/pii/S0306454915005551>

603

604 [20] Floyd, M., Bromley, B.P., and Pencer, J., 2017, A Canadian Perspective on Progress in  
605 Thoria Fuel Science and Technology, CNL Nuclear Review, Vol. 6, No. 1, 17 pages. Free  
606 download from: <https://pubs.cnl.ca/doi/full/10.12943/CNR.2016.00016>

607

608 [21] Bromley, B.P., 2021, Initial Exploratory Reactor Physics Assessment of Non-  
609 Conventional Fuel Concepts for Very Compact Small Modular Reactors Using Hydroxides  
610 as Coolants and/or Moderators, ANS Nuclear Technology Journal, May. Free download  
611 from: <https://www.tandfonline.com/doi/full/10.1080/00295450.2021.1874778>

612

613

614

### Figure Captions List

615

- Fig. 1 Core layout of MHTGR-350 (Adapted from Fig. 3 from [11])
- Fig. 2 Reference fuel block layout (Adapted from Fig. 2-2 from [12])
- Fig. 3 Radial cross section view of fuel element geometry (not to scale)
- Fig. 4 Modified HTGR Fuel Block Concept with Moderator Elements
- Fig. 5 Calculated values of  $k_{inf}$  from the benchmark and reference models
- Fig. 6 Normalized neutron energy spectrum ( $n \cdot cm^{-2} \cdot s^{-1} / \text{total flux}$ ) for the reference (TRISO particles in fuel compact) and annular pellet uranium-based oxycarbide fuel concepts
- Fig. 7  $k_{inf}$  of the reference (TRISO particles in fuel compact) and annular pellet uranium-based oxycarbide fuel concepts
- Fig. 8 Neutron leakage of the reference (TRISO fuel compact) and annular pellet uranium oxycarbide fuel concepts
- Fig. 9  $k_{eff}$  of the reference (TRISO fuel compact) and annular pellet uranium oxycarbide fuel concepts
- Fig. 10 Exit burnup of the reference (TRISO fuel compact) and annular pellet uranium oxycarbide fuel concepts
- Fig. 11 Fuel residence time of the reference (TRISO fuel compact) and annular pellet uranium oxycarbide fuel concepts
- Fig. 12 NU consumption of the reference (TRISO fuel compact) and annular pellet uranium oxycarbide fuel concepts
- Fig. 13 Fuel Temperature Reactivity Coefficient (FTRC) of the reference (TRISO fuel compact) and annular pellet uranium oxycarbide fuel concepts
- Fig. 14 Graphite Moderator Temperature Reactivity Coefficient (GTRC) reference (TRISO fuel compact) and annular pellet uranium oxy-carbide fuel concepts
- Fig. 15 Comparison of  $k_{eff}$  for the uranium and uranium-thorium annular fuel pellet concepts

616

617

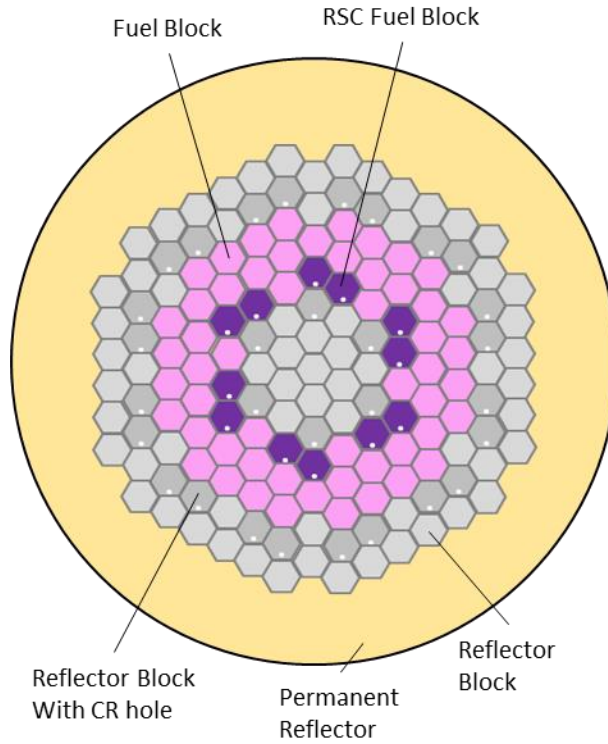
**Table Caption List**

618

Table 1	Specifications for TRISO Particles (adapted from Table 2-2 from [12])
Table 2	Reference fuel compact and block specifications (from [12])
Table 3	Assumed Material Temperatures of HTGR Components
Table 4	Reference composition of UC0.5O1.5 (from [13])
Table 5	Description of regions in heterogeneous annular fuel element
Table 6	Fuel Specifications for Annular Fuel Pellet Concepts
Table 7	Uranium and thorium oxy-carbide isotopic compositions (g/cm <sup>3</sup> )
Table 8	Burnups and temperatures that are used to calculate reactivity coefficients
Table 9	Cross-section and thermal scattering data
Table 10	Annular concepts core fuel mass
Table 11	Hydrogen-based Moderator Temperature Reactivity Coefficient (HTRC) of the annular pellet uranium oxy-carbide fuel concepts
Table 12	Comparison of burnup, residence time and NU consumption for the uranium and uranium-thorium annular fuel pellet concepts
Table 13	Comparison of temperature reactivity coefficients for the uranium and uranium-thorium annular fuel pellet concepts

619

620



621

622

\* Note: there are 12 fuel columns with RCS Fuel Blocks (Purple).

623

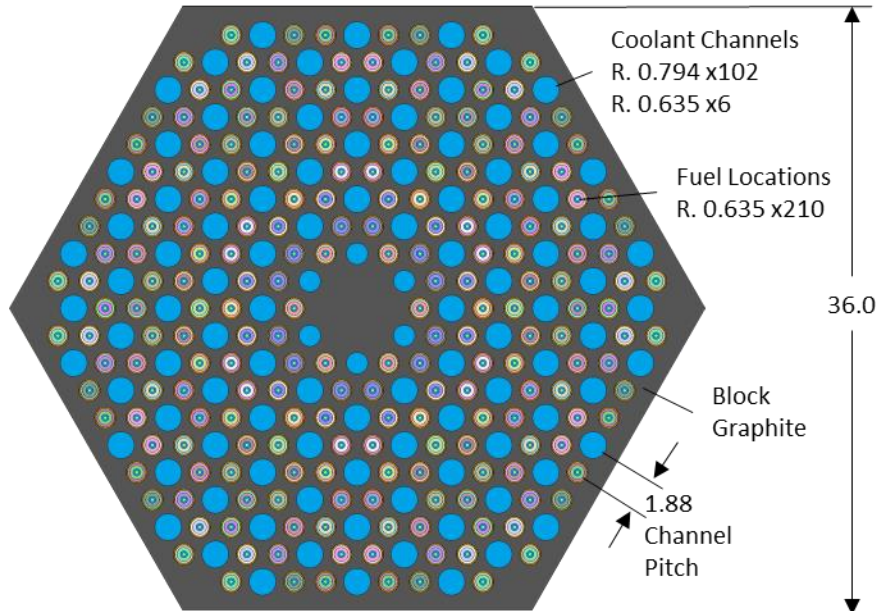
There are 6 (inner ring) + 24 (middle ring) + 24 (outer ring) = 54 fuel columns with regular Fuel Blocks (Pink).

624

**Fig. 1: Core layout of MHTGR-350 (Adapted from Fig. 3 from [11])**

625

626



627

628 \*Note: There are 102 large coolant holes (0.793 cm in diameter), and 6 small coolant holes (0.635 cm in diameter).  
629 There are 210 fuel holes, each 0.635 cm in diameter. To a first approximation, there is one coolant hole for every  
630 two fuel holes.

631

**Fig. 2: Reference fuel block layout (Adapted from Fig. 2-2 from [12])**

632

633

634

635

**Table 1: Specifications for TRISO Particles (adapted from Table 2-2 from [12])**

Properties	Value	Unit
Particle layer outer radii		
Kernel	0.02125	cm
Buffer	0.03125	cm
IPyC	0.03525	cm
SiC	0.03875	cm
OPyC	0.04275	cm
Particle layer densities		
Kernel	10.9	g/cm <sup>3</sup>
Buffer	1.0	g/cm <sup>3</sup>
IPyC	1.9	g/cm <sup>3</sup>
SiC	3.2	g/cm <sup>3</sup>
OPyC	1.9	g/cm <sup>3</sup>
Particle packing fraction	0.35	

636

637

638

**Table 2: Reference fuel compact and block specifications (from [12])**

<b>Properties</b>	<b>Value</b>	<b>Unit</b>
Fuel compact radius	0.625	cm
Fuel compact height	4.928	cm
Power per compact	172	W
Fuel compact hole radius	0.635	cm
Number of fuel compact holes	210	
Large coolant hole radius	0.794	cm
Number of large coolant holes	102	
Small coolant hole radius	0.635	cm
Number of small coolant holes	6	
Block hexagon flat-to-flat length	36.0	cm

639

640



641

642

**Table 3: Assumed Material Temperatures of HTGR Components\***

Material	Temperature (K)
Fuel Compact (TRISO particles and compact graphite)	875
Helium in gap surrounding fuel compacts	855
Block graphite	835
Helium in coolant channels	750
Lithium hydride (7LiH) in alternative HTGR design**	835

643

\* Note: Temperature data are taken from reference [13], which are averaged and rounded to the nearest 5 K

644

645

646

647

\*\* As a conservative approximation, the 7LiH is assumed to be at the same temperature as the graphite block, although it is anticipated that the equilibrium 7LiH temperature will be somewhere between that of the graphite block and the helium coolant. The temperature of the 7LiH (750 K to 835 K) is well below its melting point (~965 K).

648

649

650

**Table 4: Reference composition of  $UC_{0.5}O_{1.5}$  (from [13])**

Isotope	Wt.%
U-235	13.78
U-238	75.11
O-16	8.97
C (natural)	2.14

651

652

653

**Table 5: Description of regions in heterogeneous annular fuel element**

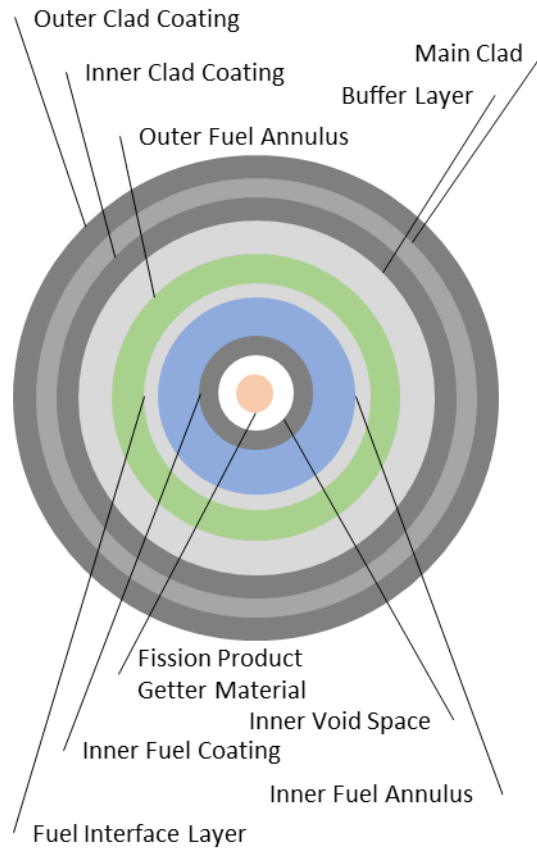
<b>Region</b>	<b>Materials</b>	<b>Outer Radius (cm)</b>	<b>Inner Radius (cm)</b>
<b>1. Outer Clad Coating</b>	Pyrolytic Carbon (OPyC)	0.625	0.621
<b>2. Main Clad</b>	Silicon Carbide (SiC)	0.621	0.561
<b>3. Inner Clad Coating</b>	Pyrolytic Carbon (IPyC)	0.561	0.557
<b>4. Buffer Layer</b>	Low Density Carbon Buffer	0.557	0.547
<b>5. Outer Fuel Annulus</b>	(U,Th)CO (see Table 6)	0.547	0.417
<b>6. Fuel Interface Layer</b>	Low Density Carbon Buffer	0.417	0.413
<b>7. Inner Fuel Annulus</b>	(U,Th)CO (see Table 6)	0.413	0.213
<b>8. Inner Fuel Coating</b>	Pyrolytic Carbon	0.213	0.209
<b>9. Inner Void Space</b>	Vacuum	0.209	0.109
<b>10. Fission Product Getter Material</b>	Porous Graphite	0.109	0

654

655

656

657



658

659

660

661

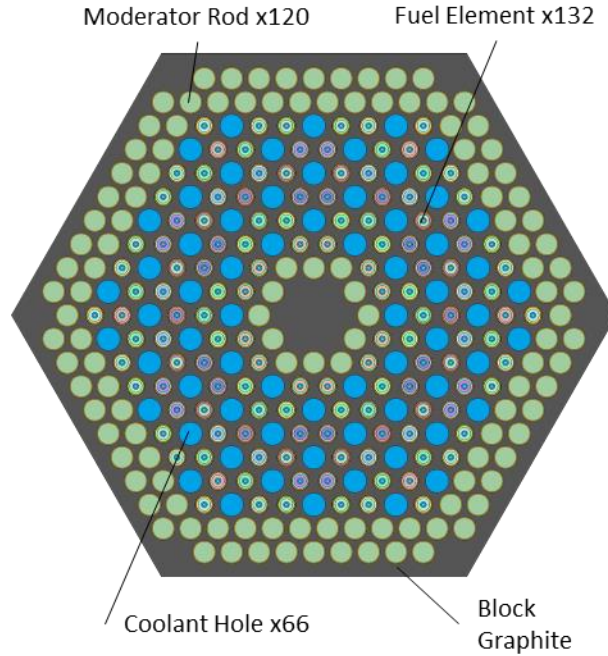
662

663

\* Note: Diagram is not to scale. Radial thickness of various coatings and clad regions and other non-fuel regions are exaggerated for better visual understanding.

**Fig. 3: Radial cross section view of fuel element geometry (not to scale)**

664



665

666 \* Green rods represent fuel and coolant holes that have been filled with a hydrogen-based moderator, such as  
667 <sup>7</sup>LiH. There are 108 Moderator holes on the outside, and 12 Moderator holes on the inside.

668 \*\* There are 132 Fuel Holes, and 66 Coolant Holes (Blue). The fuel holes are filled with heterogeneous, annular  
669 fuel pellets instead of TRISO-based fuel compacts

670

**Fig. 4: Modified HTGR Fuel Block Concept with Moderator Elements**

671

672

673

**Table 6: Fuel Specifications for Annular Fuel Pellet Concepts**

Fuel Type	Homogeneous or Heterogeneous	Outer Annulus	Inner Annulus
<b>A5</b>	Homogeneous*	LEU (5 wt.% U-235/U)	LEU (5 wt.% U-235/U)
<b>A10</b>	Homogeneous*	LEU (10 wt.% U-235/U)	LEU (10 wt.% U-235/U)
<b>A19.75</b>	Homogeneous*	HALEU (19.75 wt.% U-235/U)	HALEU (19.75 wt.% U-235/U)
<b>U10 Th</b>	Heterogeneous **	LEU (10 wt.% U-235/U)	Th
<b>U19.75 Th</b>	Heterogeneous **	HALEU (19.75 wt.% U-235/U)	Th
<b>U19.75+Th</b>	Homogeneous*	50 vol% HALEU (19.75 wt.% U-235/U), 50 vol% Th	50 vol% HALEU (19.75 wt.% U-235/U), 50 vol% Th
<b>U19.75 DU+Th</b>	Heterogeneous **	HALEU (19.75 wt.% U-235/U)	90 vol% Th, 10 vol% DU (0.2 wt.% U-235/U)

674

\* Homogeneous – Inner & Outer fuel annuli are made of the same material

675

\*\* Heterogeneous – Outer fuel annulus contains higher fissile content. Inner fuel annulus contains low fissile, high fertile content.

676

677

678  
 679

**Table 7: Uranium and thorium oxy-carbide isotopic compositions (g/cm<sup>3</sup>)**

Nuclide	Density of Nuclide in Fuel Material					
	UCO 5 wt.% U-235/U	UCO 10 wt.% U-235/U	UCO 19.75 wt.% U-235/U	ThCO	(U,Th)CO	(DU,Th)CO
<b>Th-232</b>				8.66E+00	4.33E+00	7.80E+00
<b>U-234</b>	3.71E-03	7.42E-03	1.47E-02	0.0	7.33E-03	1.48E-05
<b>U-235</b>	4.88E-01	9.76E-01	1.93E+00	0.0	9.64E-01	1.95E-03
<b>U-238</b>	9.26E+00	8.78E+00	7.82E+00	0.0	3.91E+00	9.74E-01
<b>C</b>	1.94E-01	1.95E-01	1.95E-01	1.77E-01	1.86E-01	1.79E-01
<b>O-16</b>	9.45E-01	9.45E-01	9.46E-01	8.60E-01	9.03E-01	8.68E-01
<b>O-17</b>	3.82E-04	3.82E-04	3.82E-04	3.47E-04	3.65E-04	3.51E-04
<b>Total</b>	1.09E+01	1.09E+01	1.09E+01	9.70E+00	1.03E+01	9.82E+00

680  
 681

\* What is shown in the table is the mass density (in g/cm<sup>3</sup>) of each isotope in each fuel material

682 **Table 8: Burnups and temperatures that are used to calculate reactivity coefficients**

<b>Material</b>	<b>Burnup fraction<sup>a</sup></b>	<b>Material Temperatures (K)</b>
Fuel	0, 1/3, 2/3, 1	600, 900, 1200, 1500
Graphite	0, 1/3, 2/3, 1	300, 600, 900, 1200
Hydrogen-based Moderator <sup>b</sup>	0, 1/3, 2/3, 1	300, 600, 900, 1200

<sup>a</sup> Zero (0) burnup fraction corresponds to fresh fuel, and burnup fraction of 1 corresponds to the exit burnup.

<sup>b</sup> Hydrogen-based moderator compact. Note that the melting point of <sup>7</sup>LiH is 688°C (961 K), and the boiling point is ~950°C (1,223 K)

683



684

**Table 9: Cross-section and thermal scattering data**

<b>Material Temperature (K)</b>	<b>Cross-section Data (temperature)*</b>	<b>Thermal Scattering Data (temperature)</b>
300	*.03c (300 K)	gre7.00t (294 K)
600	*.06c (600 K)	gre7.12t (600 K)
900	*.09c (900 K)	gre7.18t (800 K)
1200	*.12c (1200 K)	gre7.22t (1200 K)
1500	*.15c (1500 K)	gre7.22t (1200 K)

685

Note: \* is the name of the isotope. For example, 92225.03c is the data file for U-235 evaluated at 300 K.

686

687

**Table 10: Annular concepts core fuel mass**

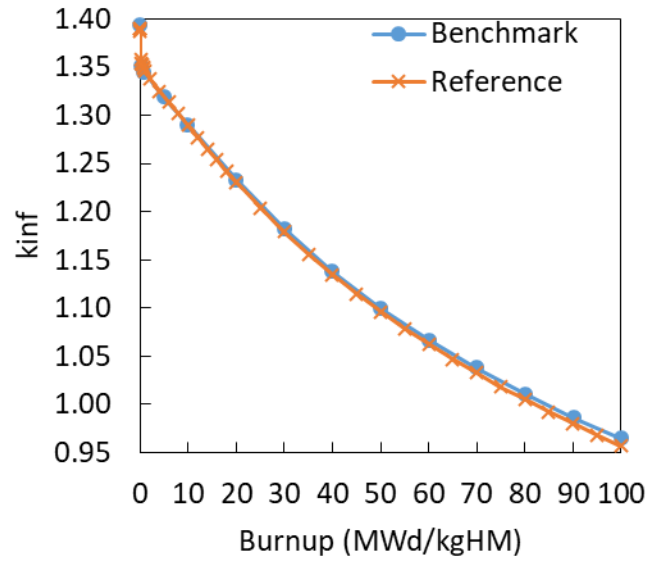
Mass of Fuel in Core with Fuel Type (refer to Table 6)							
Element	Uranium Fuel			Uranium-Thorium Fuel			
	A5	A10	A19.75	U10 Th	U19.75 Th	U19.75+Th	U19.75 DU+Th
<b>U (kgU)</b>	47969	47966	47960	23995	23991	23980	23991*
<b>Th (kgTh)</b>				21278	21278	21288	19150
<b>Total (kgHM)</b>	47969	47966	47960	45272	45269.	45268	45539

688

\* DU is not included here.

689

690



691

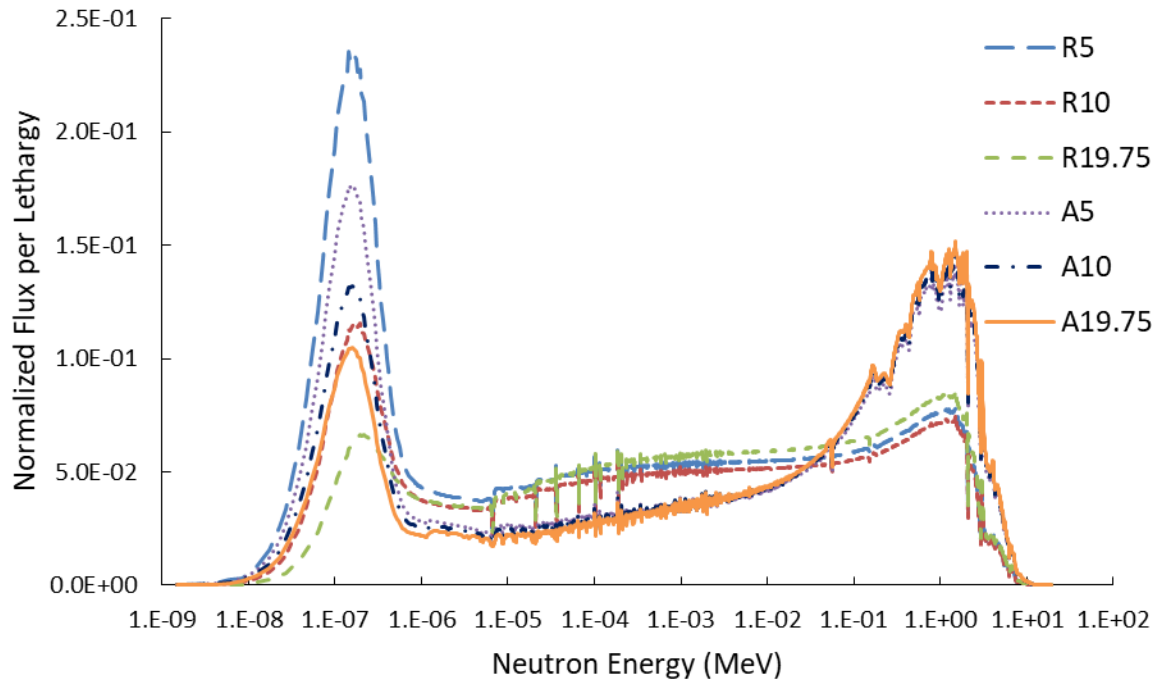
692

**Fig. 5: Calculated values of  $k_{inf}$  from the benchmark and reference models**

693

694

695



696

697 \* Notice that R19.75, which uses TRISO fuel compacts with 19.75 wt% U-235/U, has a neutron energy spectrum  
698 that is beginning to resemble a fast-spectrum reactor, due to a lower C/U-235 ratio, and insufficient moderation.

699 **Fig. 6: Normalized neutron energy spectrum ( $n \cdot \text{cm}^{-2} \cdot \text{s}^{-1} / \text{total flux}$ ) for the reference (TRISO  
700 particles in fuel compact) and annular pellet uranium-based oxycarbide fuel concepts**

701

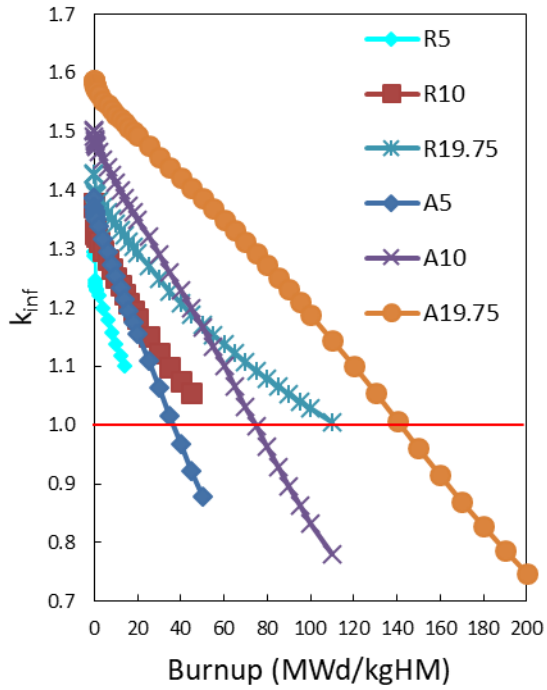
702

703

704

705

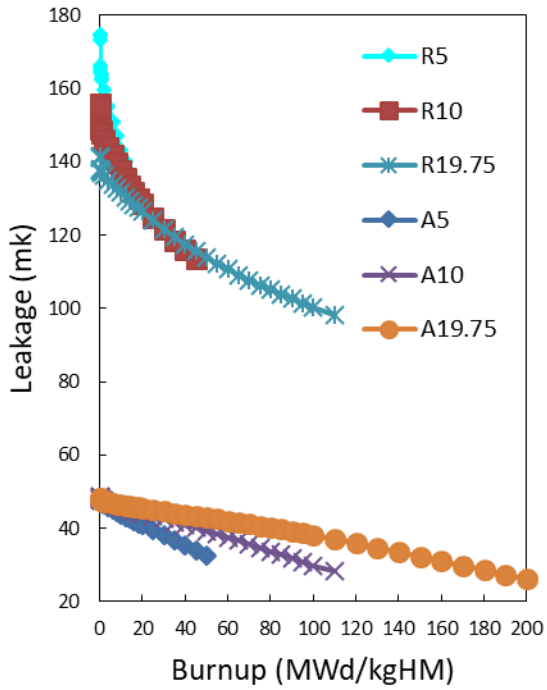
706



707

708 **Fig. 7:  $k_{inf}$  of the reference (TRISO particles in fuel compact) and annular pellet uranium-based**  
709 **oxycarbide fuel concepts**

710



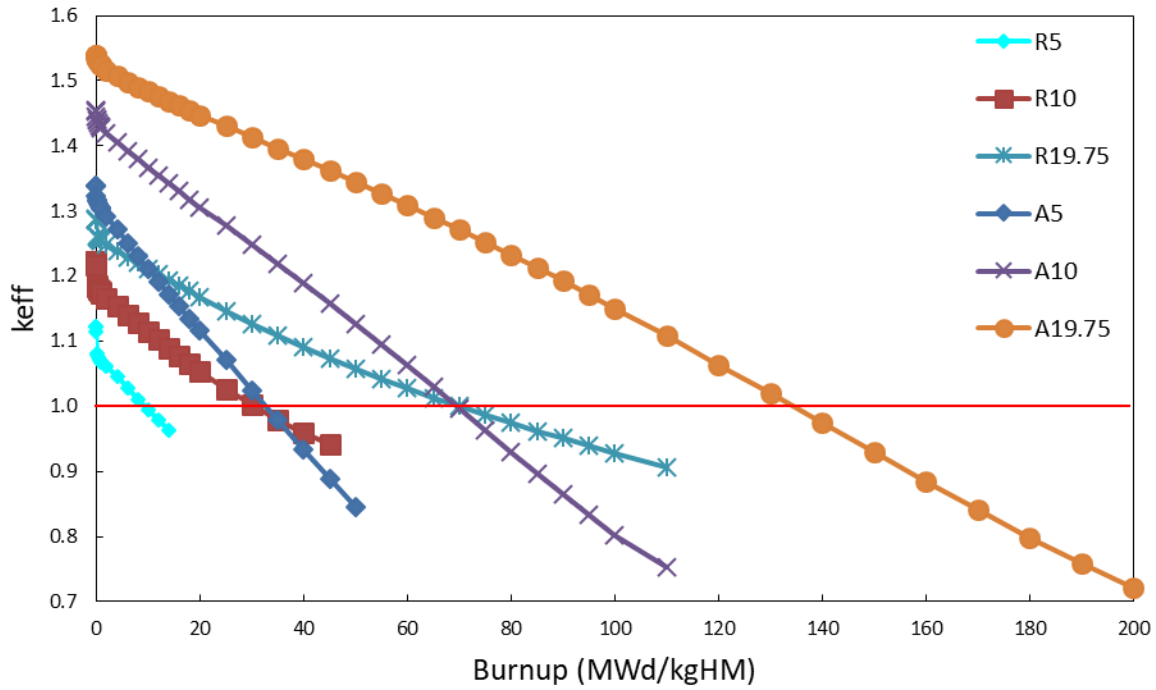
711

712

713

714

**Fig. 8: Neutron leakage of the reference (TRISO fuel compact) and annular pellet uranium oxycarbide fuel concepts**



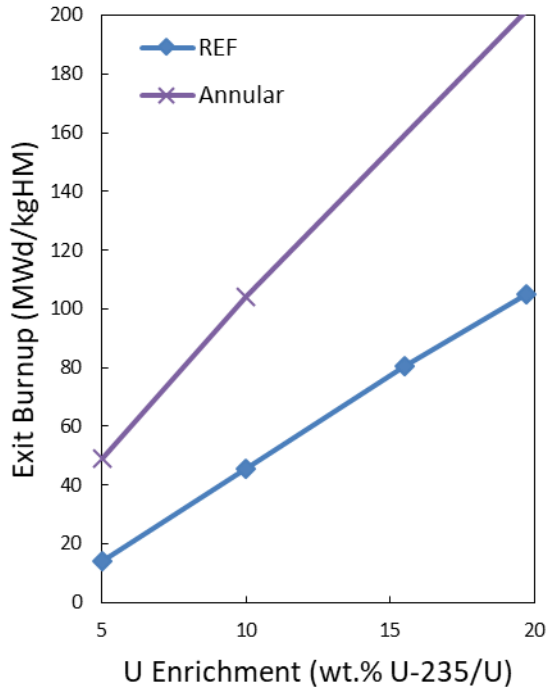
715

716

717

718

**Fig. 9:  $k_{eff}$  of the reference (TRISO fuel compact) and annular pellet uranium oxycarbide fuel concepts**



719

720

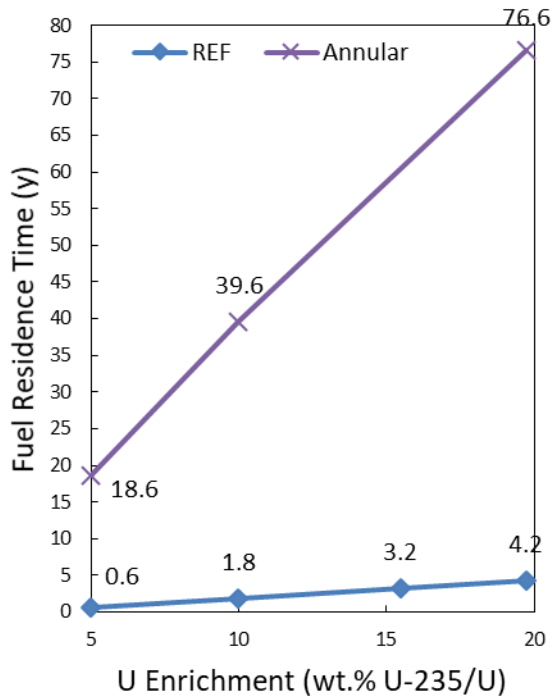
721

722

**Fig. 10: Exit burnup of the reference (TRISO fuel compact) and annular pellet uranium oxycarbide fuel concepts**



723



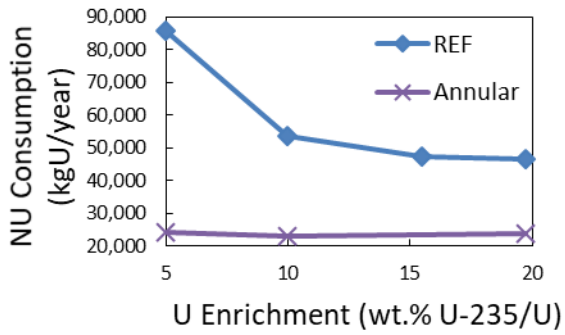
724

725 **Fig. 11: Fuel residence time of the reference (TRISO fuel compact) and annular pellet uranium**  
726 **oxycarbide fuel concepts**

727

728

729



730

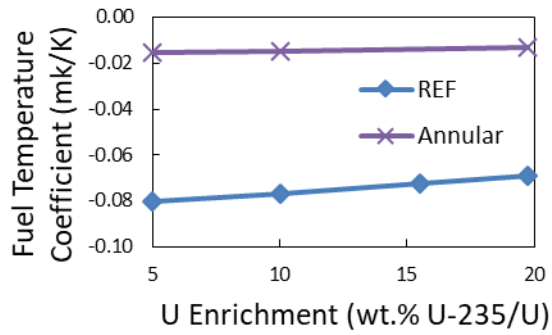
731

732

**Fig. 12: NU consumption of the reference (TRISO fuel compact) and annular pellet uranium oxycarbide fuel concepts**

733

734



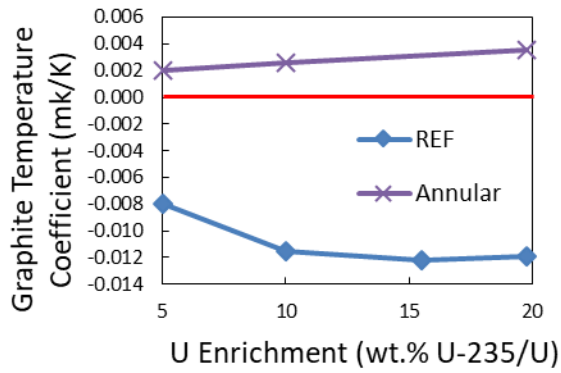
735

736 \* Note: The FTRCs shown in this plot are averaged over burnup and fuel temperature.

737 **Fig. 13: Fuel Temperature Reactivity Coefficient (FTRC) of the reference (TRISO fuel compact)**  
738 **and annular pellet uranium oxycarbide fuel concepts**

739

740



741

742 \* Note: The GTRCs shown in this plot are averaged over burnup and graphite temperature.

743 **Fig. 14: Graphite Moderator Temperature Reactivity Coefficient (GTRC) reference (TRISO fuel**  
744 **compact) and annular pellet uranium oxy-carbide fuel concepts**

745

746

747

748

**Table 11: Hydrogen-based Moderator Temperature Reactivity Coefficient (HTRC) of the annular pellet uranium oxy-carbide fuel concepts**

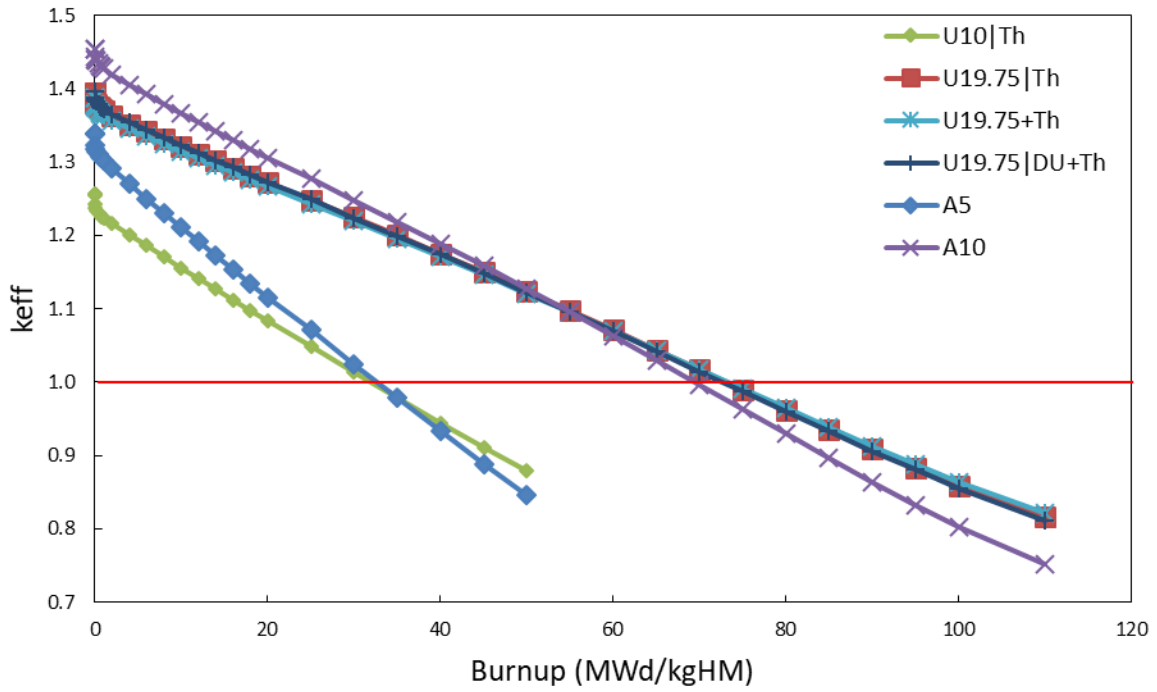
wt.% U-235/U	HTRC (mk/K)
5	0.094
10	0.088
19.75	0.085

749

\* Note: The HTRCs shown in this table are averaged over burnup and hydrogen temperature.

750

751



752

753 **Fig. 15: Comparison of  $k_{eff}$  for the uranium and uranium-thorium annular fuel pellet concepts**

754

755

756 **Table 12: Comparison of burnup, residence time and NU consumption for the uranium and**  
757 **uranium-thorium annular fuel pellet concepts**

Fissile Content	Concept	Burnup (MWd/kgHM)	Residence Time (y)	NU Consumption (MTU/y)
5 wt.% U-235/HM	A5	49.0	18.6	24.2
	U10 Th	47.9	17.2	26.7
10 wt.% U-235/HM	A10	104.2	39.6	23.2
	U19.75 Th	109.6	39.3	23.3
	U19.75+Th	109.8	39.4	23.3
	U19.75 DU+Th	108.9	39.3	23.3

758

759

760 **Table 13: Comparison of temperature reactivity coefficients for the uranium and uranium-**  
761 **thorium annular fuel pellet concepts**

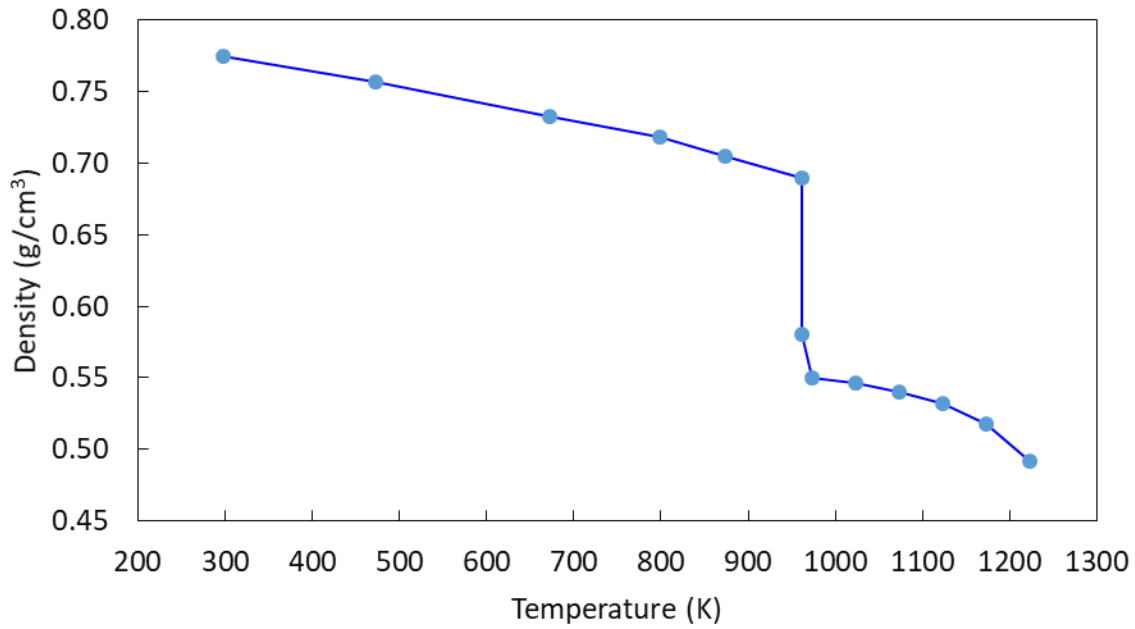
Fissile Content	Concept	FTRC (mk/K)	GTRC (mk/K)	HTRC (mk/K)
5 wt.% U-235/HM	A5	-0.016	0.002	0.094
	U10 Th	-0.022	0.002	0.087
10 wt.% U-235/HM	A10	-0.015	0.003	0.088
	U19.75 Th	-0.021	0.002	0.083
	U19.75+Th	-0.022	0.002	0.083
	U19.75 DU+Th	-0.021	0.002	0.083

762 \* Note: The temperature coefficients shown in this table are averaged over burnup and temperature.

763



764



765

766 \* Note: the melting point of LiH is ~692°C / 965 K

767 **Fig. 16: Density Variation with Temperature for Lithium Hydride (data obtained from [18])**

768

769